

## Interface of *n*-type WSe<sub>2</sub> photoanodes in aqueous solution. I. Electrical properties

R. Bourezg, G. Couturier, and J. Salardenne

*Laboratoire d'Etude des Matériaux pour la Microélectronique, Université de Bordeaux 1, 351 Cours de La Libération, 33405 Talence CEDEX France*

F. Lévy

*Institut de Physique Appliquée, Ecole Polytechnique Fédérale de Lausanne, CH-1015 Lausanne, Switzerland*

(Received 30 December 1991; revised manuscript received 1 July 1992)

Transport properties of *n*-type WSe<sub>2</sub> single crystals and dark electrical properties of a polyiodide aqueous electrolyte/*n*-type WSe<sub>2</sub> interface are reported in this paper. The conductivity anisotropy ( $\sigma_{\parallel}/\sigma_{\perp}$ ) has been measured versus the temperature, it is found practically temperature independent but sample dependent; suggestions are made about the conduction across the layers. Electrical properties of the electrolyte/semiconductor interface were investigated by various methods such as *I-V*, *C-V*, *G-V*, and admittance spectroscopy. Perpendicular electrodes with various surface conditions and electrodes parallel to the *c* axis were studied in order to better understand the role played by surface defects such as steps. It is shown, for example, that much caution has to be taken in interpreting *C-V* measurements of stepped electrodes. Our results indicate that the conductivity anisotropy greatly enhances the electronic transfers occurring through the steps.

### I. INTRODUCTION

During these past years, much work has been devoted to the study of the transition-metal chalcogenides (WSe<sub>2</sub>, MoSe<sub>2</sub>, MoTe<sub>2</sub>, . . .) as semiconductor electrodes in photoelectrochemical (PEC) cells. These materials were first identified by Tributsch and co-worker<sup>1,2</sup> to have a large photoconversion efficiency, a good stability in solution, and also to match the solar spectrum well. These layer-type semiconductors are constituted by sheets in the sequence *X-M-X, X-M-X, . . .*, where *M* stands for the metal. Within each layer the metal is bonded to six nearest-neighbor chalcogen *X* atoms by covalent forces; between each layers van der Waals forces are predominant. The bonding between layers is weak and thus a large anisotropy of some physical properties, such as the electrical conductivity, are expected.<sup>3</sup> Beside defects introduced by impurities, these materials usually have stacking defects which can strongly modify the intrinsic properties, as we will see in the following. Due to the weak interaction between the sheets these materials show an easy cleavage, but the surface is not free of defects (dislocations and steps are the main defects). It has been shown that the photoconversion efficiency depends on the surface conditions,<sup>4-6</sup> and it is generally assumed that dangling bonds on the surface  $\parallel$  to the *c* axis act as recombination centers, damaging the quantum efficiency.<sup>7</sup> Single crystals usually have small areas, so an alternative would be the use of thin films which can be obtained with large areas. Recent works have shown that stoichiometric polycrystalline films can be grown but here again surfaces of these films have a large density of defects leading to a very poor efficiency.<sup>8-10</sup>

Thus it is of great interest to understand the electronic transfer mechanisms occurring at the surface defects like steps. Several papers have already been devoted to this

subject, but due to the large disparity of results it is not easy to have a clear opinion on this subject.

In this paper, we report mainly electrical results concerning the bulk and interface properties of electrodes  $\parallel$  and  $\perp$  to the *c* axis. The experimental procedure is described in Sec. II. Section III deals with the bulk properties deduced from Hall measurements versus the temperature. Section IV is devoted to the properties of the electrolyte/WSe<sub>2</sub> interface. Various techniques such as current-voltage, capacitance-voltage, conductance-voltage, and admittance spectroscopy were used to investigate this interface.

Optical and photoelectrochemical properties are reported in the following paper and they are discussed on the basis of the electrical results presented in this first paper.

Numerous samples have been tested in our experiments, but it seems to us that all the samples have roughly the same behavior in so far as they have the same surface quality. Most of the results shown below were obtained with the same sample but with various surface conditions, i.e., as-grown, cleaved, and scratched cleaved. This has the advantage that it eliminates the differences of morphology occurring between several samples grown at the same time.<sup>11</sup>

### II. EXPERIMENTAL SECTION

*n*-type WSe<sub>2</sub> single crystals were grown by the chemical-vapor transport technique with various transporting agents.<sup>12</sup> The crystal face exposed to the electrolyte was always the (0001) van der Waals surface. Smooth electrodes  $\perp$  to the *c* axis were obtained after cleavage by peeling off the upper sheet layers of the crystal with an adhesive tape. Observation by optical microscopy showed that these surfaces were almost free of surface defects.

Measurements were done in a conventional three-electrode cell, a platinum foil being used as a counter electrode and an aqueous standard calomel electrode (SCE) as the reference electrode. The area of the Pt foil ( $\approx 40 \text{ cm}^2$ ) may be considered infinite with regard to that of the semiconductor electrode. An Ohmic contact using the In-Ga alloy was made on the back side of the sample. The sample was encapsulated in a resin so that only the surface under test of the semiconductor was exposed to the electrolyte solution. Electrodes  $\parallel$  to the *c* axis were obtained by cutting and polishing samples which were completely encapsulated in a resin.

Polyiodide ( $2\text{MKI} + 5 \times 10^{-3} \text{MI}_2$ ) aqueous electrolyte was prepared with reagent-grade chemicals (Merck) and ultrapure Millipore-Q water.

Admittance spectra were obtained from a fully computerized Solartron 1174 frequency response analyzer. Capacitance-voltage (*C-V*) and conductance-voltage (*G-V*) characteristics were obtained from a PAR (Model 124) lock-in amplifier.

### III. BULK PROPERTIES

The conductivity, the carrier concentration, and the mobility of various single crystals were measured in the temperature range 77–500 K. All the samples being *n* type, Ohmic contacts were performed with the In-Ga alloy. Before measurements the samples were cleaved in order to have a uniform thickness; an ac Van der Pauw method was used.<sup>13</sup>

Typical curves of conductivity ( $\sigma_{\perp}$ ) and carrier concentration along the layers are given in Fig. 1. All the samples give roughly the same results. The dopant concentration is about  $5 \times 10^{16} \text{ cm}^{-3}$  and their activation energy is 97 meV; at room temperature the carrier concentration is  $3.5 \times 10^{16} \text{ cm}^{-3}$ . The mobility curve shown in Fig. 2 is fitted well by a temperature power law like  $\mu = AT^{-\gamma}$  with  $\gamma = 2.42$  and  $A = 1.46 \times 10^8 \text{ cm}^2 \text{ V}^{-1} \text{ s}^{-1} \text{ K}^{\gamma}$ . The  $\gamma$  exponent agrees very well with the usual value found for this material.<sup>3</sup> We point out that a good fit is also obtained by using a law such as  $B(e^{\theta/T} - 1)$  with  $\theta = 386 \text{ K}$  and  $B = 60 \text{ cm}^2 \text{ V}^{-1} \text{ s}^{-1}$ . Both laws confirm that scattering by optical phonons is the main diffusion process in this layered material.<sup>13-16</sup>

The transverse conductivity across the layers ( $\sigma_{\perp}$ ) was

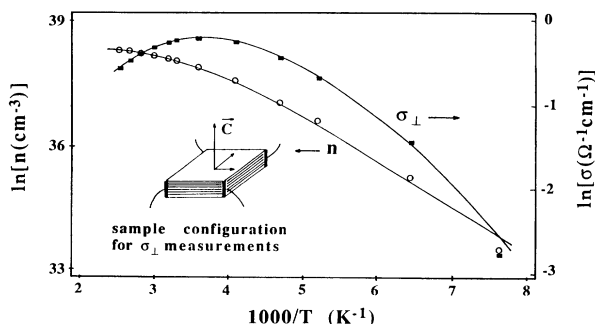


FIG. 1. Logarithms of the conductivity and carrier concentration measured along the layers vs  $1000/T$ .

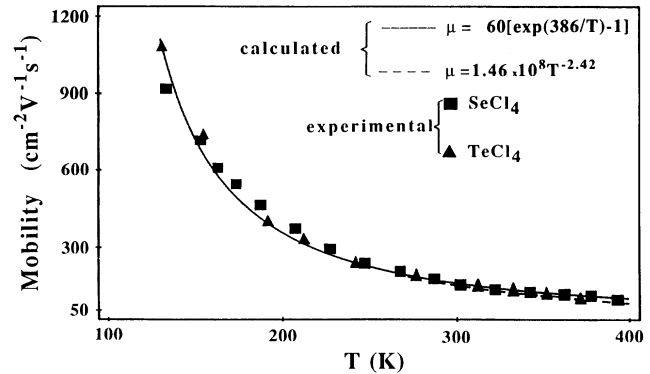


FIG. 2. Experimental and theoretical mobility curves along the layers vs  $T$ .

measured for various samples. The Montgomery method<sup>17</sup> was used to deduce the  $\sigma_{\parallel}$  value. Measurements were difficult because samples were very thin (30–300  $\mu\text{m}$ ). As shown in Fig. 3,  $\sigma_{\parallel}$  varies greatly from one sample to another whereas  $\sigma_{\perp}$  is the same for all samples. The  $\sigma_{\parallel}/\sigma_{\perp}$  ratio varies from  $3 \times 10^{-2}$  to  $3 \times 10^{-4}$ . The large range of variation of  $\sigma_{\parallel}/\sigma_{\perp}$  tends to indicate that the measured conductivity across the layers is not an intrinsic property of the WSe<sub>2</sub> material related to the effective-mass anisotropy but must be related to defects. Moreover, the fact that the temperature dependences of  $\sigma_{\parallel}$  and  $\sigma_{\perp}$  are nearly the same suggests that in both cases the carriers are mainly moving along the layers, the electron transfers from one layer to the other needed in the  $\sigma_{\parallel}$  case taking place at special sites randomly distributed.

A model for the conductivity anisotropy of layered semiconductors has been proposed<sup>3,18,19</sup> on the basis of the results obtained in GaSe material. In this model the  $\sigma_{\parallel}/\sigma_{\perp}$  ratio is not controlled by the effective-mass ratio which is not very different from one but by stacking defects which lead to a localization of the electronic states in the *c* axis direction. The anisotropy is then well described by a law such as  $A \exp(-\Delta E/kT)$  where  $A$  is the effective-mass ratio and  $\Delta E$  is the mobility edge re-

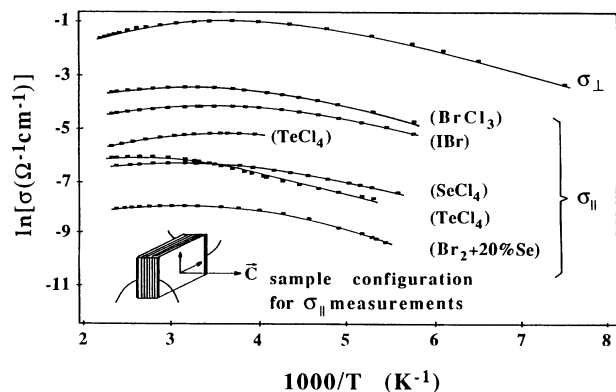


FIG. 3.  $\sigma_{\perp}$  and  $\sigma_{\parallel}$  vs  $1000/T$  for various samples grown with different transport agents,  $\text{BrCl}_3$ ,  $\text{IBr}$ ,  $\text{TeCl}_4$ ,  $\text{SeCl}_4$ , and  $\text{Br}_2 + 20\% \text{ Se}$ .

sulting from the stacking defects. Our results show a too-large value of the  $\sigma_{\parallel}/\sigma_{\perp}$  ratio with a too-small temperature dependence to be described by this model alone.

Finally, the electron localization by stacking defects cannot be excluded but another mechanism leading to least resistance paths has also to be considered. This latter one permits to electrons with energy smaller than  $\Delta E$  and thus partially localized to be transferred from one layer to another.

In the following, the reported results are related to samples grown with  $\text{SeCl}_4$  as the transport agent.

#### IV. ELECTRICAL PROPERTIES OF THE ELECTROLYTE/WSe<sub>2</sub> INTERFACE

The electrical properties of the electrolyte/*n*-type WSe<sub>2</sub> interface were investigated by current-voltage (*I-V*) capacitance-voltage (*C-V*), and conductance-voltage (*G-V*) characteristics and also by admittance spectroscopy. Electrodes  $\perp$  and  $\parallel$  to the *c* axis were studied. All the measurements were performed in darkness.

##### A. *I-V* characteristics

The *I-V* characteristics are shown in Fig. 4; curves *a*, *b*, and *c* correspond to electrodes  $\perp$  to the *c* axis and curve *d* to an electrode  $\parallel$  to the *c* axis; the voltage sweep rate was  $1 \text{ mV s}^{-1}$ . An uncleaved electrode with a large amount of steplike defects has a large reverse current, as shown in curve *a*. The reverse current becomes very weak for a smooth electrode nearly free of defects, as shown in curve *b*. The electrodes were obtained by cleaving with an adhesive tape. Curve *c* was obtained after scratching a smooth electrode; the reverse current is then strongly enhanced by the presence of steps. For electrodes  $\parallel$  to the *c* axis the reverse current is very high and its slope  $\Delta V/\Delta I$  is slightly higher than the value of the bulk resistance  $r_b$  ( $r_b^{-1} = \sigma_{\parallel} S/e$  where *S* and *e* are respectively the area and the thickness of the sample). Thus, the electrolyte/WSe<sub>2</sub> interface behaves nearly like an Ohmic contact. We have also observed that the interface resis-

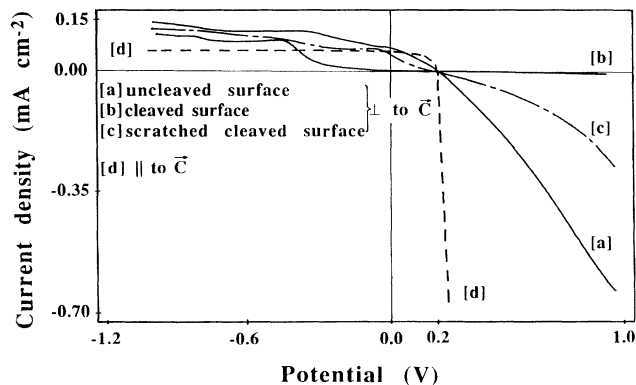


FIG. 4. *I-V* characteristics of electrodes  $\perp$  and  $\parallel$  to the *c* axis; for curve *d* multiply the scale by 50 for  $V > 0.2 \text{ V}$  and by 7 for  $V < 0.2 \text{ V}$ . The potential *V* is referenced to the SCE, the sweep rate is  $1 \text{ mV s}^{-1}$ .

tance may be increased after oxidizing the electrode.<sup>20</sup> As a conclusion of these *I-V* measurements, it is clear that the steps on the electrodes  $\perp$  to the *c* axis are paths for important leak currents and are mainly responsible for the reverse current.

The *I-V* characteristic of a smooth electrode, curve *b*, has a step at about  $-0.5 \text{ eV}$ ; it will be shown later that this value corresponds to the flat band condition in the semiconductor. The *I-V* characteristic is nearly the same as one of a perfect Schottky diode except that the forward current is limited at about  $10^{-4} \text{ A cm}^{-2}$ . This remark stands for all the electrodes,  $\parallel$  or  $\perp$  to the *c* axis. The *I-V* characteristic of Pt/electrolyte/Pt also exhibits a similar limitation.<sup>21</sup> Thus, the reaction  $2e^- + \text{I}_2 \rightarrow 2\text{I}^-$  occurring at the WSe<sub>2</sub> electrode may be invoked as the limiting process because of the diffusion of  $\text{I}_2$  in the solution. There are at least two reasons for that assumption: (1) the direct current is proportional to the  $\text{I}_2$  concentration; (2) a diffusional impedance is revealed by admittance spectroscopy.

##### B. Admittance spectroscopy and *C-V* characteristics

The frequency dependence of the admittance of the electrolyte/WSe<sub>2</sub> interface has been studied. Real,  $Y_r(\omega)$ , and imaginary,  $Y_i(\omega)$ , parts of the total admittance  $Y(\omega) = Y_r(\omega) + iY_i(\omega)$  of electrodes  $\parallel$  and  $\perp$  to the *c* axis are shown, respectively, in Figs. 5 and 6. Measurements shown here were done under a zero bias voltage between the Pt counter electrode and the WSe<sub>2</sub> semiconductor, i.e.,  $V_{\text{SC/SCE}} = 0.2 \text{ V}$ , where SC denotes semiconductor and SCE denotes standard calomel electrode. Results discussed below were obtained with the same samples which were used in the *I-V* measurements.

##### 1. Electrodes $\parallel$ to the *c* axis

Because electrodes  $\perp$  to the *c* axis always have steps on the surface, we first examine the case of electrodes  $\parallel$  to the *c* axis. Results can be discussed with the help of the electrical network drawn in the inset in Fig. 5; this circuit does not allow an exact fit to the data, but it is a good approach to aid in the understanding of the electrical prop-

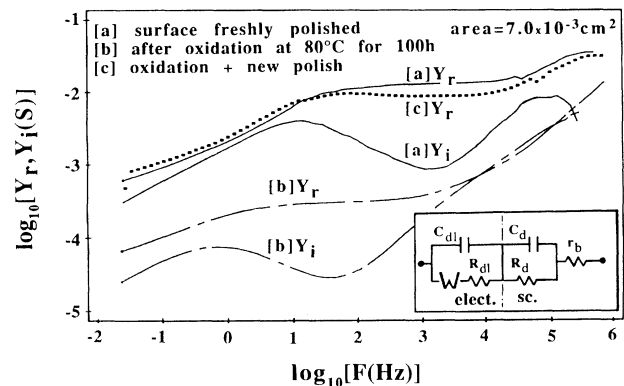


FIG. 5. Real  $Y_r$  and imaginary  $Y_i$  parts of the admittance of an electrode  $\parallel$  to the *c* axis. The inset shows the electrical network used to obtain the data.

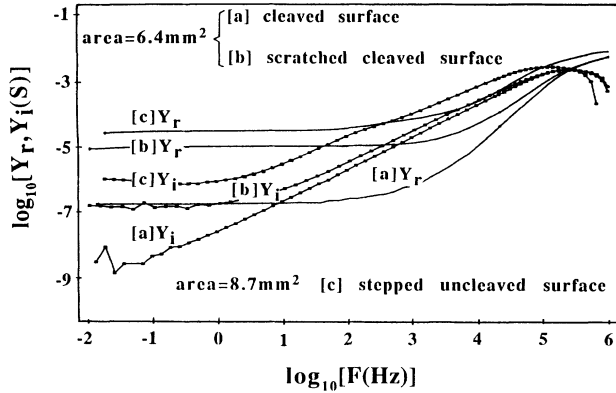


FIG. 6. Real  $Y_r$  and imaginary  $Y_i$  parts of the admittance of an electrode  $\perp$  to the  $c$  axis.

erties of the interface in the frequency range of the study.  $C_{dl}$  and  $C_d$  are the double-layer capacitance and the depletion layer capacitance of the semiconductor,  $R_{dl}$  and  $R_d$  are the transfer resistances through the double layer and the depletion layer,  $W$  is a diffusional impedance (Warburg impedance), and  $r_b$  is the bulk resistance of the semiconductor.

At high frequencies  $Y_r(\omega) \approx 1/r_b$ , where  $r_b$  is the bulk resistance of the sample. A value of the conductivity along the layer may be deduced from  $r_b$  by calculating the quantity  $e/Sr_b$  where  $e$  and  $S$  are the thickness and the area of the sample, respectively. The value found by this method is in good agreement with  $\sigma_{\perp}$  measured by the Van der Pauw method.

At lower frequencies around  $10^4$  kHz, the capacitance  $Y_i(\omega)/\omega \approx 35$  nF, i.e.,  $5 \mu\text{F cm}^{-2}$ , a value far larger than the capacitance measured for a cleaved surface as we will see later. This capacitance is of the same order of magnitude than classical double-layer capacitances ( $\approx 10 \mu\text{F cm}^{-2}$ ) thus it corresponds to  $C_{dl}$  in the electrical network. For the same range of frequency,  $Y_r(\omega)$  reaches a plateau and its value depends only of the electrode area, thus it is assigned to  $R_{dl}$  the transfer resistance through the double layer,  $R_{dl} = 70 \Omega$  for an area of  $7 \times 10^{-3} \text{ cm}^2$ . It was verified that  $R_{dl} + r_b$  is equal to the  $\Delta V/\Delta I$  slope of the reverse  $I$ - $V$  characteristic because for this regime the diffusion is not the limitative process.

For very low frequencies, say below 10 Hz,  $Y_r(\omega)$  and  $Y_i(\omega)$  decrease with the same slope, close to  $1/2$ . Thus the expressions for  $Y_r(\omega)$  and  $Y_i(\omega)$  take the form of a diffusional admittance  $A(i\omega)^{1/2}$ . This admittance is assigned to ion diffusion in the electrolyte and is observed because of the low value of the transfer resistance  $R_d$ .

For parallel electrodes it seems that the transfer resistance  $R_d$  can be nearly neglected, thus the depletion layer capacitance of the semiconductor is not observed. A pinning of the Fermi level by a large density of states at the interface is the simplest way to account for that situation. Defects at the interface may be either metal-induced gap states<sup>22-25</sup> (MIGS) or states resulting from a chemical reaction at the semiconductor surface.<sup>26,27</sup> As a consequence, near the surface the semiconductor is in accumu-

lation or very weak depletion thus the potential drops mainly through the double layer and therefore the resulting barrier height is very small. There is no need to invoke a band-edge shift or a change of the electronic affinity in the semiconductor to explain the situation at a step as discussed by various authors.<sup>28</sup> This hypothesis is inconsistent with the fact that band edges of WSe<sub>2</sub> are energetically stable in the presence of different redox coupled and concentrations.<sup>29</sup>

The situation described here, except for the diffusion process, is very similar to the case of a Schottky diode with a very thin insulating layer and a pinning of the Fermi level by a large density of states.<sup>30</sup>

$Y_r(\omega)$  and  $Y_i(\omega)$  of an oxidized electrode are also reported in Fig. 5. The oxidation was performed at a temperature of  $80^\circ\text{C}$  for 100 h. The increase of the transfer resistance and the decrease of the capacitance which result from that process may be enhanced not only by the growth of a thin insulating layer at the surface but also by a reduction of the surface defect density. After a new polish of the surface,  $Y_r(\omega)$  and  $Y_i(\omega)$  again have their initial values.

## 2. Electrodes $\perp$ to the $c$ axis

We now discuss the case of electrodes  $\perp$  to the  $c$  axis. The results can be interpreted on the basis of the same electrical network previously used. However, the effects of the double-layer capacitance and of the diffusional impedance are little or not at all observed because the electronic transfers at the interface become very small at zero bias voltage.

At high frequencies the bulk resistance  $r_b$  of the stepped uncleaved electrode is slightly smaller than those of cleaved or scratched cleaved electrodes because the sample area was reduced after cleaving in order to eliminate steps at the area periphery, reduction of the thickness by peeling off having little importance. The value of  $r_b$  is in good agreement with the one calculated by using the  $\sigma_{\parallel}$  conductivity.

At low frequencies  $Y_r(\omega)$  reaches a constant value  $1/(R_d + r_b)$  where  $R_d$  is ascribed to the electron transfer through the depletion layer in the semiconductor. The value of  $R_d$  is strongly dependent on the surface conditions;  $R_d$  decreases as the amount of steps on the surface increases. In Fig. 6, it is seen that  $R_d$  increases by 2 orders of magnitude after a cleaving,  $R_d = 7.5 \times 10^6 \Omega$  for an area of  $6.4 \times 10^{-2} \text{ cm}^2$ .

For a smooth electrode,  $Y_i(\omega)$  behaves approximatively as a pure capacitance for frequencies lower than  $10^4$ - $10^5$  Hz. This is shown in Fig. 7, where the plot  $Y_i(\omega)/\omega$  is nearly a constant. The capacitance corresponds to the depletion layer capacitance  $C_d$  of the semiconductor, ( $C_d = 17$  nF, i.e.,  $0.26 \mu\text{F cm}^{-2}$ ). Thus a plot of  $1/C^2$  vs  $V_{SC/SCE}$  performed at frequencies smaller than  $10^4$ - $10^5$  Hz allows us to determine the concentration  $N_D$  of donor atoms and the built-in potential  $V_{bi}$  which are given by the slope of  $1/C^2$  vs  $V_{SC/SCE}$  and by the voltage axis intercept, respectively, as shown in Fig. 8 ( $N_D \approx 2 \times 10^{16} \text{ cm}^{-3}$  and  $V_{bi} \approx 0.7$  V, i.e.,  $0.5 \text{ V} + 0.2 \text{ V}$ ). These values are in good agreement with the results given

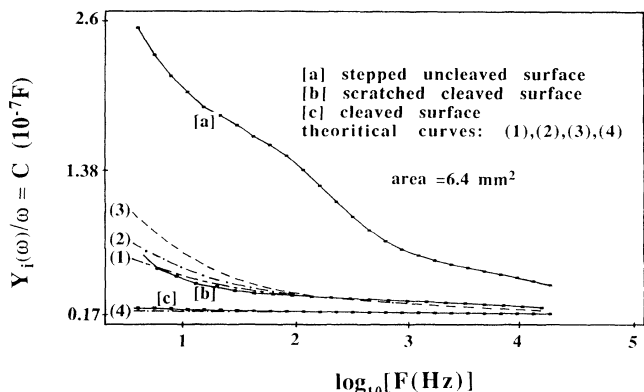


FIG. 7. Experimental and calculated  $Y_i(\omega)/\omega$  for various states of the surface of an electrode  $\perp$  to the  $c$  axis. Curve (1):  $C_0 = 3 \times 10^{-10}$  F,  $R_0 = 2$  k $\Omega$ ,  $C_1 = 8 \times 10^{-7}$  F,  $a = 1.25$ ; curve (2):  $C_0 = 6 \times 10^{-10}$  F,  $R_0 = 1$  k $\Omega$ ,  $C_1 = 8 \times 10^{-7}$  F,  $a = 1.25$ ; curve (3):  $C_0 = 15 \times 10^{-10}$  F,  $R_0 = 400$   $\Omega$ ,  $C_1 = 8 \times 10^{-7}$  F,  $a = 1.25$ ; curve (4):  $C_0 = 0$ ,  $R_0 = \infty$ ,  $C_1 = 8 \times 10^{-7}$  F. Forty elementary cells have been used in the calculations.

by Hall measurements and  $I$ - $V$  characteristics. In Fig. 8, three plots of  $1/C^2$  vs  $V_{SC/SCE}$  are given which correspond respectively to 20 kHz, 2 kHz, and 200 Hz. It is observed that the slope depends slightly on the frequency measurement. As we will see later, this reveals that the surface is not completely free of defects.

For stepped uncleaned and scratched cleaned electrodes  $Y_i(\omega)$  is no longer a simple capacitance as shown by the plots of  $Y_i(\omega)/\omega$  (see Fig. 7). There are two reasons for this behavior: (1) at low frequencies, below about 1 Hz, the increase of  $Y_i(\omega)/\omega$  is due to the double-layer capacitance  $C_{dl}$  of the electrolyte; (2) from about  $10^4$  to 1 Hz, the weak increase of  $Y_i(\omega)/\omega$  (see Fig. 7) is undoubtedly due to the presence of steps. Thus, a rather more complicated network than the one drawn in Fig. 5 is necessary to fit the admittance curves of stepped uncleaned and scratched cleaned electrodes. This point now has to be discussed.

Because the contact is nearly Ohmic on the surface of a

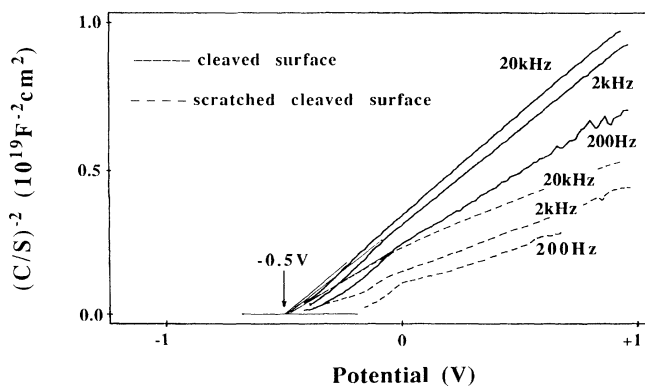


FIG. 8. Plots of  $1/C^2$  vs  $V_{SC/SCE}$  at various frequencies for a cleaved and scratched-cleaved electrode  $\perp$  to the  $c$  axis. The potential  $V$  is referenced to the SCE, the sweep rate is  $1$  mV s $^{-1}$ .

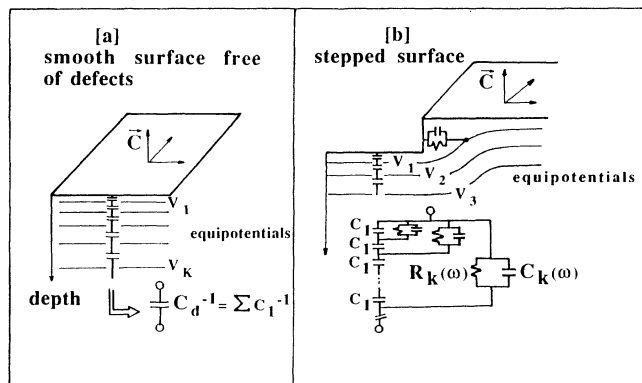


FIG. 9. Electrical networks of a cleaved smooth and scratched cleaved electrode  $\perp$  to the  $c$  axis.

step which is  $\parallel$  to the  $c$  axis, the equipotentials are strongly modified in the vicinity of the step. In particular, due to the conductivity anisotropy ( $\sigma_{\perp} \gg \sigma_{\parallel}$ ) the potential along the layers parallel to the surface is kept to the surface potential. A schematic representation of the potential drop near a step is sketched in Fig. 9(b). As a consequence, at frequencies where the admittance was normally well described by the sole depletion layer capacitance of the layers  $\perp$  to the  $c$  axis we now have to take into account the admittance corresponding to the surface of the step  $\parallel$  to the  $c$  axis. As shown in Fig. 9(b), each equipotential is now connected to the surface via a  $R_k(\omega) \parallel C_k(\omega)$  cell, where the subscript  $k$  stands for the  $k^{eme}$  equipotential; this results from the admittance studies of electrodes  $\parallel$  to the  $c$  axis. To further extend the model, we need a law for  $R_k$  and  $C_k$ . As a first attempt, we tried a simple law which verifies that  $R_k$  and  $C_k^{-1}$  increase as the subscript  $k$  increases, assuming that  $k=0$  for the nearest equipotential from the surface. We chose  $R_k = R_{k=0} a^k$  and  $C_k = C_{k=0} a^{-k}$ . The calculated and experimental curves of  $Y_i(\omega)/\omega$  are plotted in Fig. 7 for various values of  $R_{k=0} = R_0$  and  $C_{k=0} = C_0$ . The agreement between experimental and theoretical curves could probably be improved by a more sophisticated model but the rather coarse approach used here allows us to bring out the role played by a step on an electrode  $\perp$  to the  $c$  axis.

For stepped surfaces, no information as to the carrier concentration or the built-in potential can be obtained from the  $1/C^2$  vs  $V_{SC/SCE}$  plots, because the measured capacitance is not the true depletion layer capacitance. This fact is illustrated in Fig. 8, where three  $1/C^2$  vs  $V_{SC/SCE}$  plots recorded at 20 kHz, 2 kHz, and 200 Hz are shown. These plots are not perfectly straight lines and cause some difficulties in determining for instance the built-in potential. Moreover, an apparent high value of the carrier concentration is obtained. Thus much caution has to be taken in interpreting these  $C$ - $V$  characteristics.

C.  $G$ - $V$  characteristics

The presence of steps on an electrode  $\perp$  to the  $c$  axis may be seen clearly by  $G$ - $V$  measurements. This tech-

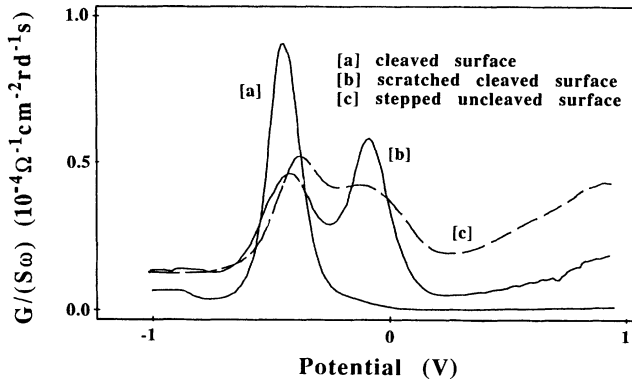


FIG. 10.  $G$ - $V$  characteristics of an electrode  $\perp$  to the  $c$  axis for three different states of the surface. The potential  $V$  is referenced to the SCE, the sweep rate is  $1 \text{ mV s}^{-1}$ .

nique is very powerful to investigate, for instance, electronic states at insulating material/semiconductor interfaces or in the depletion region of Schottky diodes.<sup>31,32</sup> For an ideal diode free of defects, the conductance is zero for reverse bias and increases towards a limiting value  $r_b^{-1}$  for direct bias and no conductance peak is expected. The situation here is slightly different because of the current limitation imposed by the reaction  $2e^- + \text{I}_2 \rightarrow 2\text{I}^-$  at the WSe<sub>2</sub> electrode.

The  $GV$  characteristics are shown in Fig. 10. The curves  $a$ ,  $b$ , and  $c$  correspond to a cleaved, scratched cleaved, and stepped uncleaved electrode, respectively. In the case of a cleaved surface, the  $G$ - $V$  plot exhibits a peak at a voltage corresponding to the flat band condition in the semiconductor, i.e., at  $V_{\text{SC/SCE}} = -0.5 \text{ V}$ , as predicted by the  $1/C^2$  vs  $V_{\text{SC/SCE}}$  plot. After scratching the surface of the electrode, a second peak occurs at  $V_{\text{SC/SCE}} = -0.09 \text{ V}$  (see curve  $b$ ). Of course, it must be attributed to the steps due to the scratching, i.e., the part of the interface which is  $\parallel$  to the  $c$  axis. This is in good agreement with the fact that the height of the barrier for an electrode  $\parallel$  to the  $c$  axis is very small; this point has already been discussed above. We may reasonably assume that the magnitude of a conductance peak is still proportional to the area of the electrode as in a classical  $G$ - $V$  characteristic. Although the scratched area is very small ( $\approx 0.5 \text{ mm}^2$ ) in regard to the total area ( $6.4 \text{ mm}^2$ ), the peak at  $-0.5 \text{ V}$  of the curve  $b$  is 2 times smaller than before scratching, as if the effective area of the electrode  $\perp$  to the  $c$  axis was considerably reduced. This behavior is well supported by the fact that a step strongly modifies the equipotentials in its vicinity. Consequently a large area around the step is practically put in contact with the electrolyte via the small area of the step, because of (1) the large conductivity  $\sigma_{\perp}$  along the layer and (2) the nearly Ohmic contact on surface  $\parallel$  to the  $c$  axis.

The whole area under either the two or the sole conductance peaks, respectively, for scratched cleaved or cleaved surfaces is unchanged. Hence, this area can be expressed as

$$\int_{0.2V}^{-1V} G(x) dx = \int dI = C^{te},$$

where  $G(V) = dI/dV$  at low frequencies. The constant value of the current at negative bias confirms that the forward current is limited by the diffusion rate of the  $\text{I}_2$  species in the solution and not by the state of the surface.

## V. CONCLUSION

Transport measurements show that  $\sigma_{\parallel}$  has roughly the same temperature dependence as  $\sigma_{\perp}$ . The  $\sigma_{\perp}/\sigma_{\parallel}$  ratio is not an intrinsic property and is not related to the effective-mass anisotropy. The model of stacking defects which works well for some layered semiconductors like GaSe cannot describe our results alone; another mechanism has to be considered.

Electrical properties of the  $2\text{MKI} + 5 \times 10^{-3}\text{MI}_2$  electrolyte/WSe<sub>2</sub> interface have been studied by various methods as admittance spectroscopy,  $I$ - $V$ ,  $C$ - $V$ , and  $G$ - $V$  characteristics. Electrodes  $\parallel$  to the  $c$  axis behave nearly like Ohmic contacts.

The interface impedance of electrodes  $\perp$  to the  $c$  axis is strongly dependent on the surface conditions. Cleaved smooth electrodes nearly free of defects have a Schottky behavior at reverse bias. The diffusion potential  $V_{\text{bi}}$  is deduced from the  $1/C^2$  vs  $V_{\text{SC/SCE}}$  plot. Also deduced from this plot is the carrier concentration, its value being in very good agreement with that found by Hall measurements in bulk material. The  $G$ - $V$  characteristics of these electrodes exhibit one conductance peak at a voltage  $V_{\text{SC/SCE}} = V_{\text{bi}}$ . This was interpreted on the basis of a limited diffusion rate of the  $\text{I}_2$  species in the electrolyte.

Electrodes with surface defects like steps have an important reverse current and the admittance spectroscopy results suggest that the equipotentials near a step are strongly modified. This is due to the fact that the surface of the step  $\parallel$  to the  $c$  axis is nearly an Ohmic contact and also because  $\sigma_{\perp} \gg \sigma_{\parallel}$ . Experimental results are roughly described by using a simple network of distributed  $R_k(\omega) \parallel C_k(\omega)$  cells. For these electrodes, the  $G$ - $V$  characteristics show two peaks, one situated at  $V_{\text{SC/SCE}} = V_{\text{bi}}$  and a second one at  $V_{\text{SC/SCE}} = -0.09 \text{ V}$ , the former still being due to the part of the surface  $\perp$  to the  $c$  axis and the latter to the surface of the step which is  $\parallel$  to the  $c$  axis. Although the area of the step is very small compared to the total area of the electrode, it can be observed that the magnitude of the conductance peak at  $V_{\text{bi}}$  is strongly reduced. As a conclusion of that, it seems that a small defect can, in a coarse approximation, put a large area of the electrode in "Ohmic contact" with the electrolyte. This behavior brings out large troubles for the photoconversion efficiency, a point which is more extensively detailed in the next paper.

## ACKNOWLEDGMENTS

The authors would like to thank Dr. J. N. Chazalviel from PMC-Ecole Polytechnique-Paris, for a very helpful discussion about admittance spectroscopy results.

- <sup>1</sup>H. Tributsch, Ber. Bunsenges, Phys. Chem. **81**, 361 (1977); **82**, 169 (1978).
- <sup>2</sup>H. Tributsch and J. S. Bennet, J. Electroanal. Chem. **81**, 97 (1977); H. Tributsch, *ibid.* **125**, 1086 (1978).
- <sup>3</sup>R. C. Fivaz and Ph.E. Schmid, in *Physics and Chemistry of Materials with Layered Structures*, Optical and Electrical Properties, edited by P. A. Lee (Reidel, Dordrechts, 1976), Vol. 4.
- <sup>4</sup>H. J. Lewerenz, A. Heller, and F. J. Disalvo, J. Am. Chem. Soc. **102**, 1877 (1980).
- <sup>5</sup>H. S. White, F. R. F. Fan, and A. J. Bard, J. Electrochem. Soc. **128**, 1045 (1981).
- <sup>6</sup>C. Lévy-Clément and R. Tenne, in *Photoelectrochemistry and Photovoltaics of Layered Semiconductors*, edited by A. Aruchamy (Kluwer Academic, Dordrecht, 1991).
- <sup>7</sup>H. J. Lewerenz, H. Gerischer, and M. Lübke, J. Electrochem. Soc. **131**, 100 (1984).
- <sup>8</sup>R. Bourezg, G. Couturier, and J. Salardenne, J. Chim. Phys. **88**, 2021 (1991).
- <sup>9</sup>C. R. Cabrera and H. D. Abruña, J. Electrochem. Soc. **135**, 1436 (1988).
- <sup>10</sup>C. R. Cabrera and H. D. Abruña, J. Electrochem. Soc. **129**, 673 (1982).
- <sup>11</sup>F. R. F. Fan and A.J. Bard, J. Electrochem. Soc. **128**, 945 (1981).
- <sup>12</sup>F. Lévy, Ph. Schmid, and H. Berger, Philos. Mag. **34**, 1129 (1976); F. Lévy, Nuovo Cimento B **38**, 359 (1977).
- <sup>13</sup>L. J. van der Pauw, Philips Res. Rep. **13**, 1 (1958).
- <sup>14</sup>R. Fivaz and E. Moser, Phys. Rev. **136**, A833 (1964); **163**, 743 (1967).
- <sup>15</sup>R. Fivaz, J. Phys. Chem. Solids **28**, 839 (1967).
- <sup>16</sup>F. J. Blatt, *Physics of Electronic Conduction in Solids* (McGraw-Hill, New York, 1968).
- <sup>17</sup>H. C. Montgomery, J. Appl. Phys. **42**, 2971 (1971).
- <sup>18</sup>K. Maschke and Ph. Schmid, Phys. Rev. B **12**, 4312 (1975).
- <sup>19</sup>K. Maschke and H. Overhof, Phys. Rev. B **15**, 2058 (1977).
- <sup>20</sup>R. Bourezg, G. Couturier, J. Salardenne, J. P. Doumerc, and F. Lévy, following paper, Phys. Rev. B **46**, 15 410 (1992).
- <sup>21</sup>R. Bourezg, Thèse d'Etat No. 982, Université Bordeaux 1, 1992.
- <sup>22</sup>V. Heine, Phys. Rev. **138**, A1689 (1965).
- <sup>23</sup>S. G. Louie and M. L. Cohen, Phys. Rev. B **13**, 2461 (1976).
- <sup>24</sup>S. G. Louie, J. R. Chelikowsky, and M. L. Cohen, Phys. Rev. B **15**, 2154 (1977).
- <sup>25</sup>J. Tersoff, Phys. Rev. Lett. **52**, 465 (1984); **56**, 675 (1986).
- <sup>26</sup>J. N. Chazalviel and T. B. Truong, J. Electroanal. Chem. **114**, 299 (1980).
- <sup>27</sup>J. N. Chazalviel and T. B. Truong, J. Am. Chem. Soc. **103**, 7447 (1981).
- <sup>28</sup>P. Salvador, M. Pujadas, and G. Campet, Phys. Rev. B **38**, 9881 (1988).
- <sup>29</sup>C. A. Koval and J. B. Olson, J. Phys. Chem. **92**, 6276 (1988).
- <sup>30</sup>S. M. Sze, *Physics of Semiconductor Devices* (Wiley, New York, 1981).
- <sup>31</sup>E. H. Nicollian and A. Goetzberger, Bell. Syst. Tech. J. **46**, 1055 (1967).
- <sup>32</sup>K. Lehovec, A. Slbodskoy, and J. Sprague, Phys. Status Solidi **3**, 447 (1965).